

Introducing the Dirac-Milne universe

A. Benoit-Lévy¹ and G. Chardin²

¹ Institut d'Astrophysique de Paris, 98 bis, bvd Arago, 75014 Paris, France. e-mail: benoit1@iap.fr

² CSNSM, Univ. Paris-Sud & CNRS/IN2P3, 91405 Orsay, France. e-mail: chardin@csnsm.in2p3.fr

August 16, 2022

ABSTRACT

The Λ CDM standard model, although an excellent parametrization of the present cosmological data, requires two as yet unobserved components, Dark Matter and Dark Energy, for more than 95% of the Universe. Faced to this unsatisfactory situation, we study an unconventional cosmology, the Dirac-Milne universe, a matter-antimatter symmetric cosmology, in which antimatter is supposed to present a negative active gravitational mass. The main feature of this cosmology is the linear evolution of the scale factor with time which directly solves the age and horizon problems of a matter-dominated universe. We study the concordance of this model to the cosmological test of Type Ia Supernovae distance measurements and calculate the theoretical primordial abundances of light elements for this cosmology. We also show that the acoustic scale of the Cosmic Microwave Background naturally emerges at the degree scale despite an open geometry.

Key words. Cosmology: theory - Cosmology: dark energy - primordial nucleosynthesis

1. Introduction

Inflation-based Λ CDM cosmological model represents a great achievement in modern Cosmology. Its predictions are in good agreement with a wide varieties of observational cosmological tests, ranging from Big-Bang Nucleosynthesis and Cosmic Microwave Background anisotropies to distances measurements on Type Ia Supernovae. However, this success comes at a expensive cost as two poorly-understood components are required in the theory to provide the concordance of the cosmological model to the observations. These components are, on one hand, Dark Matter, whose density is estimated around $\sim 20\%$ of the critical density and Dark Energy which accounts for as much as $\sim 75\%$ of the energy content of the Universe.

The physical nature of Dark Energy remains to be elucidated but all the cosmological observations tend to indicate that it behaves in a similar way as a vacuum energy, characterized by an equation of state $p = -\rho$, where pressure and density are equal in absolute value but opposite. Dark Energy appears therefore responsible for the acceleration of the expansion of the Universe, which tends to be confirmed notably by Type Ia Supernovae distances measurements.

Faced with this uncomfortable situation where we understand less than 5% of our Universe, we study the unconventional cosmology of a symmetric universe *i.e.* containing equal quantities of matter and antimatter, where antimatter is supposed to present a negative active gravitational mass. The main consequence of this provoking hypothesis is that at large scales, above the characteristic length of the matter-antimatter distribution, the expansion factor evolves linearly with time, reminding of the Milne cosmology (Milne 1933).

The main motivation to consider the possibility that antimatter presents a negative active gravitational mass is provided by the work of Carter (1968) on the Kerr-Newman geometry representing charged spinning black holes. As noted initially by Carter, the Kerr-Newman geometry with the mass, charge and spin of an elementary particle such as an electron bears sev-

eral of the features expected from the real corresponding particle. In particular, the Kerr-Newman “electron” has no horizon, presents automatically the $g = 2$ gyromagnetic ratio and has a ring structure with radius equal to half the Compton radius of the electron. Additionally, this geometry presents charge and mass/energy reversal symmetries that strongly evoke the CP and T matter-antimatter symmetry (Chardin 1997; Chardin & Rax 1992) : when the non-singular interior of the ring is crossed, a second \mathbb{R}^4 space is found where charge and mass change sign (Carter 1968). Therefore, starting from an electron with negative charge and positive mass as measured in the first \mathbb{R}^4 space, we find in the second space a “positron” with positive charge and negative mass. The relation of the Kerr-Newman geometry to Dirac’s equation and therefore to antimatter has been noted by some authors (Arcos & Pereira 2004; Burinskii 2008).

Introduction of negative mass is not a popular idea amongst physicists and our purpose is not to provide a demonstration that antimatter has a negative active gravitational mass. Rather, we address this question through the cosmological point of view, studying the properties of such a cosmology and deriving necessary conditions that this model must fulfill in order to comply with observational tests. Still, it is important to have in mind that an analogous system exists in condensed matter, where electrons and holes in a semiconductor appear as quasiparticles with positive inertial mass, but where holes present an energy density lower than the “vacuum” constituted by the semiconductor in its ground state, and antigravitate in a gravitational field (Tsidil’kovskii 1975).

It should also be noted that at the present day, the gravitational behavior of antimatter has not been investigated in laboratory experiments. Gravity experiments on antihydrogen are under way (Drobychev et al. 2007; Pérez et al. 2008) and are expected to bring a definitive answer on that question, hopefully within the next decade.

The paper is organized as follows. In Sects. 2 and 3, we present some general properties of the Dirac-Milne universe. Section 4 is devoted to the study of Primordial Nucleosynthesis

within the framework of the Dirac-Milne cosmology. In Sect. 5, we study the compliance of the model to Type Ia Supernovæ distance measurements. In Sect. 6, we investigate the geometric implications for CMB anisotropies and for baryonic acoustic oscillations.

2. The Dirac-Milne Universe

We consider a model in which space-time is endowed with a Friedmann-Robertson-Walker (FRW) metric, given by the usual formula:

$$ds^2 = dt^2 - a(t)^2 (d\chi^2 + \text{sink}^2 \chi d\Omega^2), \quad (1)$$

where $\text{sink} = \sin \chi, \chi, \sinh \chi$ according to the value $k = 1, 0, -1$ of the parameter k describing the spatial curvature, and $a(t)$ is the scale factor. For such a FRW metric, the time-time and space-space components of the Einstein tensor $G_{\mu\nu}$ take the following form:

$$G_0^0 = 3 \frac{\dot{a}^2 + k}{a^2} \quad G_i^i = -\frac{k + 2\ddot{a}a + \dot{a}^2}{a^2}. \quad (2)$$

At scales larger than the characteristic size of the emulsion, the presence of equal quantities of matter with positive mass and antimatter with negative mass leads to the nullity of the stress-energy tensor $T_{\mu\nu}$.

Using Einstein equation $G_{\mu\nu} = 8\pi G T_{\mu\nu}$, we therefore have the following equivalence:

$$T_{\mu\nu} = 0 \Leftrightarrow a(t) \propto t \text{ and } k = -1. \quad (3)$$

The metric of the Dirac-Milne universe then reads:

$$ds^2 = dt^2 - t^2 (d\chi^2 + \sinh^2 \chi d\Omega^2). \quad (4)$$

Like the standard Λ CDM cosmology, the Dirac-Milne universe has a distinctive geometry: while the standard Λ CDM model has a curved space-time and flat spatial sections, the Dirac-Milne universe has a flat space-time and negatively curved spatial sections.

The Friedmann equation for the Dirac-Milne universe reads:

$$H^2 = H_0^2 \left(\frac{a_0}{a} \right)^2, \quad (5)$$

where a_0 is the present value of the scale factor. Integrating this equation enables one to compute the present age of the Universe t_U :

$$t_U = \frac{1}{H_0}, \quad (6)$$

where H_0 is the Hubble constant. It should be emphasized that this is a strict equality whereas in the standard Λ CDM model, the age of the Universe is only approximatively equal to $1/H_0$. It should also be noted that the linear evolution of the scale factor solves the age problem of the Universe (Chaboyer et al. 1998), which was of prime concern before the introduction of Dark Energy, that the Dirac-Milne cosmology therefore does not require.

Using the metric in Eq. (1), the particle horizon, *i.e.*, the distance a photon can travel since the origin, is given by the following limit:

$$\lim_{t_0 \rightarrow 0} \int_{t_0}^{t_U} \frac{dt'}{a(t')}, \quad (7)$$

which diverges logarithmically in the case of the Dirac-Milne Universe. This simple fact has profound implications as it signifies that any two given places in space have been causally connected in the past. The Dirac-Milne universe therefore does not have an horizon problem and thus removes the main motivation for the introduction of inflation theories.

Therefore the linear evolution of the scale factor and the fact that the space-time is flat and spatial sections are open naturally solves two major problems in standard cosmology without requiring additional ingredients such as Dark Energy or inflation, and is an important motivation to study in detail such a cosmology.

Before presenting the properties of the Dirac-Milne universe and for the sake of clarity, we list the underlying hypothesis and necessary constraints that have been assumed so far.

1. Existence of an efficient mechanism for matter and antimatter separation. We also assume that the Dirac-Milne universe is composed of separated domains of matter and antimatter. Such universes have been abundantly studied in the context of inhomogeneous nucleosynthesis. Since this universe is matter-antimatter symmetric, this system is a percolation emulsion, meaning that the probability that a given domain extends to infinity is close to unity. The existence of an efficient mechanism leading to the formation of such an emulsion remains of course to be demonstrated. A fundamental parameter is the typical size of this emulsion. We define it as the ratio between the volume V and the surface S separating the two phases: $L = V/S$. At this stage of work, this characteristic size is a free parameter, supposed here to be a constant, that will be constrained using primordial nucleosynthesis (cf Sect. 4).
2. Antimatter has a negative active gravitational mass and there is a gravitational repulsion between matter and antimatter. This hypothesis is a necessity to avoid contact between matter and antimatter after cosmological recombination. Indeed, it has been demonstrated (Ramani & Puget 1976; Cohen et al. 1998) that in the case of a symmetric universe where antimatter is assumed to present a positive gravitational mass, the global size of domains of matter and antimatter must be of the order of the observable universe. Otherwise, annihilations at the frontiers of matter and antimatter domains would generate a diffuse gamma ray emission that would be in contradiction with observational data.
3. One of the main interests of the Dirac-Milne universe consists in providing a solution to the horizon problem without resorting to inflation. However, this fact relies on the hypothesis that the contribution of radiation to the stress-energy tensor is negligible. Indeed, if we attribute to radiation a positive contribution to the energy, the evolution of the universe will not differ significantly from the standard evolution for all epochs where the universe is radiation dominated, *i.e.* for redshifts above a few thousand. However, in presence of equal quantities of particles with positive and negative mass, this might no longer be the case. A first step toward a full demonstration that the stress-energy tensor of radiation averages to zero can be deduced from the papers by Hoyle & Narlikar (1964), in the case, studied by Hawking (1965), where the particle masses are of both signs and in equal numbers. In this case, it can be shown that the stress-energy tensor of radiation is order $1/N$ compared to its value

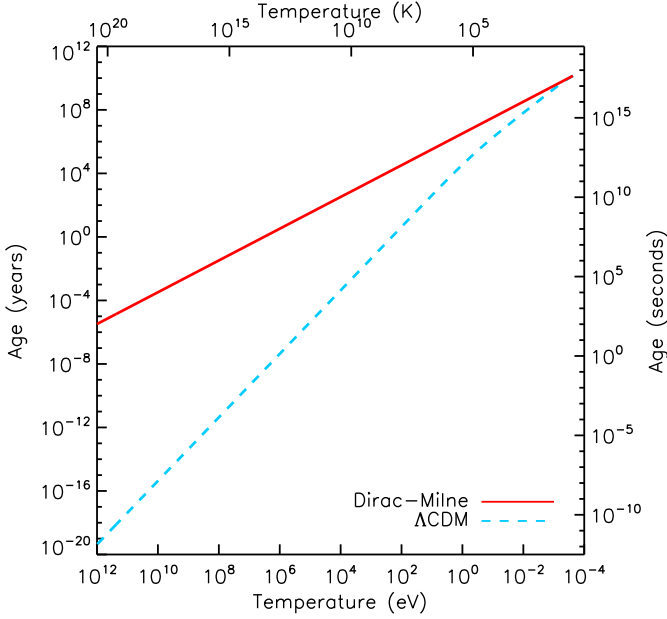


Fig. 1. Age of the Universe as a function of temperature for the Dirac-Milne universe (full line, red) and for the fiducial Λ CDM cosmology (dashed line, blue).

when all masses are of the same sign, and where N is the number of mass carriers (particles) in a Hubble horizon.

3. Some aspects of the thermal history of the Dirac-Milne Universe

Some simple properties of the Dirac-Milne universe are common with those of a purely linear cosmology as studied in Lohiya et al. (1998); Kaplinghat et al. (1999, 2000); Sethi et al. (2005). We briefly recall some of these properties.

3.1. Time-temperature relation

Using Eq. (5), it is straightforward to obtain the relation between the age of the Universe and the redshift, hence the temperature:

$$t = \frac{1}{H_0} \frac{T_0}{T}, \quad (8)$$

where T_0 is the present temperature of the Universe, as measured by CMB experiments, $T_0 = 2.725 \pm 0.001$ K (Fixsen & Mather 2002). This relation between time and temperature is valid throughout the whole history of the universe and implies that the thermal history of the Dirac-Milne universe is drastically modified as compared to the evolution in the standard Λ CDM cosmology. Figure (1) represents the age of the Universe as a function of the temperature for the Dirac-Milne and the Λ CDM models. It can be seen that, at high temperatures, the Dirac-Milne universe is much older than the corresponding Λ CDM cosmology. For instance, the traditional 1 MeV~1 sec approximation for the standard model becomes 1 MeV \sim 3.3 years in the Dirac-Milne cosmology. As noted in Lohiya et al. (1998), this difference has profound implications on Big-Bang Nucleosynthesis calculations, and will be discussed in section 4.

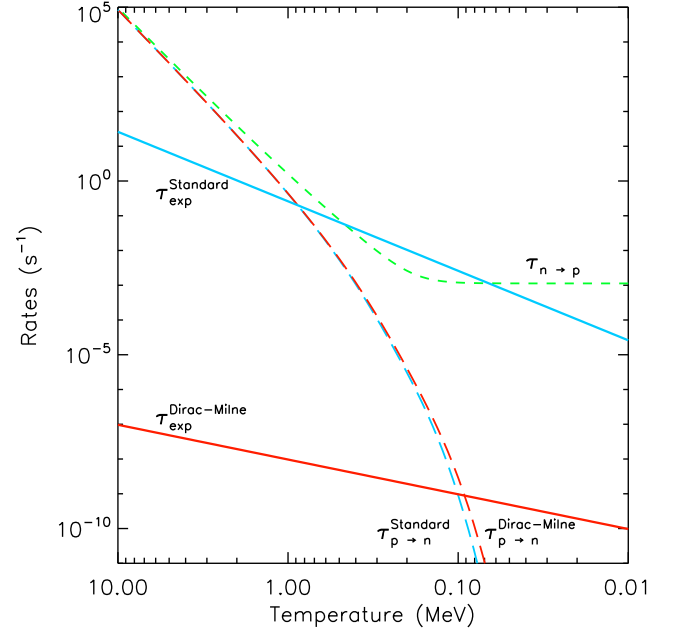


Fig. 2. Comparison between expansion rates and weak reactions rates. The short-dashed green line represents the neutron to proton conversion rate. The two solid lines represent the expansion rate of the Dirac-Milne universe (red) and of the standard cosmology (blue). The long dashed lines represent the proton to neutron conversion rates. Weak interactions decouple when these rates become lower than the expansion rate.

Another temperature of interest is the temperature of the Quark-Gluon-Plasma (QGP) transition. In Omnès model, it was proposed (Omnès 1972) that matter-antimatter separation occurred around that temperature, due to a putative repulsive interaction between nucleons and antinucleons. The maximum size of a domain of (anti)matter was controlled by the diffusion of neutrons. Aly (1974) found a maximum size of 7×10^{-4} cm at a temperature of $T \sim 330$ MeV, which was at this epoch the estimated temperature of the QGP transition. This size was found later to be in contradiction with the minimum size a domain should have in order to obtain a production of primordial helium compatible with observations (Combes et al. 1975; Aly 1978a).

The situation is rather different in the Dirac-Milne universe as the timescale at QGP transition is much larger. Since the temperature of the transition is estimated today around $T \sim 170$ MeV (Schwarz 2003), it corresponds to an age of 6×10^5 sec in the Dirac-Milne universe, a factor $\sim 10^{10}$ higher than in the standard case. This implies that the maximum size a domain could possibly grow (assuming the existence of an efficient separation mechanism) is 5 orders of magnitude higher. For this reason, the Dirac-Milne universe faces much less severe constraints than the Omnès cosmology.

3.2. Weak interactions decoupling

A fundamental example of the modifications induced by a linear scale factor resides in the epoch of decoupling of the weak interactions. This example has been treated extensively in (Lohiya et al. 1998), so we only give here the main results. In the standard model, weak decoupling occurs at a temperature $T \sim 1$ MeV.

In the Dirac-Milne universe, this decoupling happens at a lower temperature, around $T \sim 80$ keV, due to the slow variation and the low value of the expansion rate. This effect is illustrated in Fig. 2. Weak interactions control the $n \leftrightarrow p$ equilibrium. At low temperatures, this reaction is limited to the free neutron disintegration (green short-dashed line), but at temperatures higher than 80 keV, the equilibrium between proton and neutrons remains possible. The long-dashed line represent the proton conversion rate as a function of the temperature for the Dirac-Milne universe (red) and the standard cosmology (blue). The analytical expressions for these reaction rates come from Wagoner (1969); Dicus et al. (1982). Weak interactions decouple when the expansion rate becomes larger than the $p \leftrightarrow n$ rate. The small difference in the $p \leftrightarrow n$ rate between the two cosmologies stems from the fact that the neutrino background temperature differs. Indeed, as the weak interactions decouple at a temperature of $T \sim 80$ keV, neutrinos decouple from the photon background also at this temperature, but after the annihilation of most of the electron-positron pairs. This implies, as noted in Lohiya et al. (1998) that neutrinos also benefit from the entropy released by the electrons and therefore have the same temperature as the photons. The cosmic neutrino background should have a temperature equal to that of the CMB. This constitutes a distinctive feature of the Dirac-Milne universe.

4. Primordial nucleosynthesis

The primordial nucleosynthesis is a key success of the Standard Model of Cosmology. Theoretical predictions and observations are in good agreement for ${}^4\text{He}$, ${}^3\text{He}$ and D abundances, although some tensions still exist with ${}^7\text{Li}$, see Steigman (2007); Cyburt et al. (2008) for recent reviews on the topic of Standard Big-Bang Nucleosynthesis (SBBN). Given the tremendous change in the timescale (a factor $\sim 10^8$ at $T = 1$ MeV), important modifications to the traditional BBN mechanism arise (Lohiya et al. 1998; Kaplinghat et al. 1999, 2000). Primordial nucleosynthesis in the Dirac-Milne universe can be described as a two-step process: first the thermal and homogeneous production of ${}^4\text{He}$ and ${}^7\text{Li}$, and second, the production of D and ${}^3\text{He}$, the latter being one of main novelty introduced by the matter-antimatter symmetry.

4.1. Thermal and homogeneous BBN

The age of the universe at a temperature of $T \sim 80$ keV, below which deuterium is able to survive its photodisintegration, allowing the formation of ${}^4\text{He}$ nuclei, is about 40 years in the Dirac-Milne universe. This huge timescale, compared with the mean lifetime of the neutron, was first considered as an absolute obstacle to any kind of primordial helium production in a linear cosmology (Kaplinghat et al. 1999). However, it was pointed out (Lohiya et al. 1998; Kaplinghat et al. 2000) that ${}^4\text{He}$ production is in fact possible but relies on a somewhat different mechanism than the standard one.

As discussed in the previous sections, weak interactions decouple in the Dirac-Milne universe at the low temperature of $T \sim 80$ keV. This implies that the neutron and proton populations remain in thermal equilibrium until that temperature. The ratio of their densities is therefore regulated by the Boltzmann factor:

$$\frac{n}{p} = \exp\left(-\frac{Q}{T}\right), \quad (9)$$

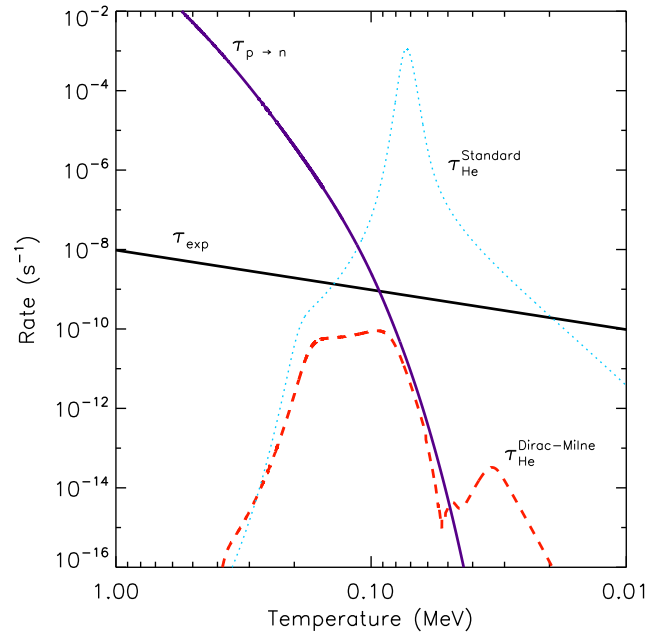


Fig. 3. ${}^4\text{He}$ production rate for the Dirac-Milne (dashed red line). The rate abruptly drops when weak interactions decouple around $T \sim 80$ keV. As a comparison, ${}^4\text{He}$ production rate for the standard BBN is also presented (dotted blue line).

where $Q = 1.29$ MeV is the difference between the neutron and proton mass.

For temperatures of the order of $T \sim 80$ keV, this number is a very small quantity ($\sim 10^{-7}$) but a few neutrons nevertheless combine with ambient protons to form deuterium, which is then incorporated in helium nuclei. As the weak interactions are still efficient, some protons inverse beta decay to neutrons, restoring the equilibrium value. Given the timescale of 40 years, this very slow process ends up in an effective production of ${}^4\text{He}$ nuclei. Fig. (3) present the production rate of ${}^4\text{He}$ in the Dirac-Milne universe (dashed line) and in the standard cosmology (dotted line). We can notice the drop in the production rate when the weak interactions decouple, leading to the nearly total disappearance of neutrons below $T \sim 80$ keV. As a simple argument showing that this mechanism leads to the right amount of ${}^4\text{He}$, we note that the product of the ${}^4\text{He}$ production rate with the Hubble time at production is roughly the same in the two models. The production rates of ${}^4\text{He}$ were obtained by calculating the time derivative of the ${}^4\text{He}$ abundances.

To compute the primordial abundances of the different light elements, we solved the non-linear systems of first-order differential equations describing the network of the nuclear reactions:

$$\frac{dY_i}{dt} = \sum_r f_{kl}^r Y_k Y_l - f_{ij}^r Y_i Y_j, \quad i = 1, N_{\text{isot}}, \quad r = 1, N_{\text{reac}}, \quad (10)$$

where Y_i is the abundance of nuclide i , N_{isot} the number of nuclides, N_{reac} the numbers of nuclear reactions included in the network, f_{ij}^r the rate of reaction $i + j \rightarrow k + l$ and f_{kl}^r the rate of reaction $k + l \rightarrow i + j$.

In order to have accurate results, it is necessary to include a large number (over a hundred) of reactions. Indeed, as the time interval during which BBN takes place is very long, some slow reactions that are ineffective during SBBN must be integrated in the nuclear reactions network for the Dirac-Milne universe

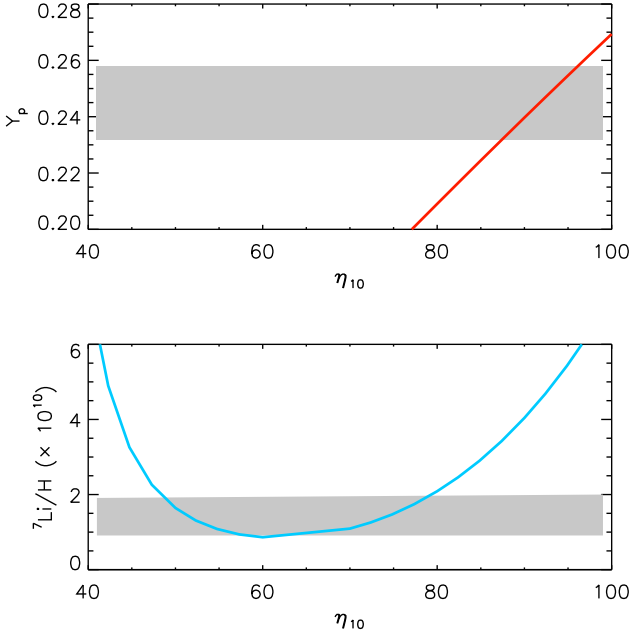


Fig. 4. ${}^4\text{He}$ (top) and ${}^7\text{Li}$ (bottom) theoretical abundances for the Dirac-Milne universe as a function of the baryon density. Here $\eta_{10} = 10^{10}\eta$. Shaded areas correspond to observational range.

(Lohiya et al. 1998). As compared to previous work on light elements production in linear cosmology (Kaplinghat et al. 2000), we used the nuclear reaction rates provided by Angulo et al. (1999); Coc et al. (2000); Tang et al. (2003); Descouvemont et al. (2004) as well as the usual rates of Wagoner (1969); Dicus et al. (1982); Caughlan & Fowler (1988); Fukugita & Kajino (1990); Rauscher et al. (1994); Chen & Savage (1999).

The precise theoretical predictions for the primordial abundances strongly depend – as in the standard case – on the baryonic density. Final primordial abundances for ${}^4\text{He}$ and ${}^7\text{Li}$ as a function of the baryonic density, characterized by the ratio η of the number of baryons to the number of photons ($\eta = n_b/n_\gamma$) are presented on figure (4). The shaded areas correspond to observational constraints (Olive & Skillman 2004; Ryan et al. 2000) on corresponding primordial abundances. The possible values for η such that the theoretical value for Y_p is compatible with the observations lie in the following range:

$$8.8 \times 10^{-9} \leq \eta \leq 9.6 \times 10^{-9}. \quad (11)$$

As can be seen in fig. (4) there is, as in the Standard Model, no value for η that allows a compatibility for ${}^4\text{He}$ and for ${}^7\text{Li}$. The lowest possible value for η yields a lithium abundance:

$$\frac{{}^7\text{Li}}{\text{H}} = 3.45 \times 10^{-10}. \quad (12)$$

Although this value is somewhat larger than the one inferred by observations, it should be noted that it is lower than the predicted value in standard cosmology calculations, namely ${}^7\text{Li}/\text{H} = (5.24^{+0.71}_{-0.67}) \times 10^{-10}$ (Cyburt et al. 2008). The Dirac-Milne universe clearly does not solve the ${}^7\text{Li}$ problem, but nevertheless alleviates it.

The value of the baryonic density inferred by the ${}^4\text{He}$ observational constraint is almost 15 times higher than the value usually admitted in the framework of standard cosmology. This

high baryonic density is a major feature of the Dirac-Milne universe as it suppresses the need for non-baryonic dark matter. Indeed, various estimates of dynamical mass all indicate a matter density in the Universe much higher than the baryonic density deduced by the BBN in the standard cosmology, which constitutes a strong motivation to postulate the existence of non-baryonic massive particles. In the Dirac-Milne universe, however, the BBN predicts a baryonic density comparable to the matter density estimated by different techniques. There is therefore no compulsory need for non-baryonic Dark Matter in the Dirac-Milne universe.

It should be noted, however, that this high value of the baryonic density aggravates the so-called missing baryon problem (Fukugita 2004). In the Standard Cosmology, this problem stems from the fact that only approximately half the baryons predicted by SBBN are observationally detected in structures. The other half is currently believed to be in the Warm-Hot Intergalactic Medium (WHIM) (Bregman 2007). In the context of the Dirac-Milne universe, this WHIM would have to be the major source of baryons. Such a possibility remains to be investigated. It should also be noted that attempts to explain dynamical behavior of galaxies resorting to cold molecular (baryonic) gas instead of non-baryonic Dark Matter have been performed in the past (Pfenniger et al. 1994) and such scenarios would need to be revisited in the new light of the Dirac-Milne model.

Figure 5 presents the evolution of the primordial abundances for the light elements as a function of the temperature for a baryonic density $\eta = 8.8 \times 10^{-9}$. It can be seen that D and ${}^3\text{He}$ are almost totally destroyed during the stage of thermal production of ${}^4\text{He}$. This fact was considered fatal to linear cosmologies (Kaplinghat et al. 2000). Although it is indeed the case for a regular linear cosmology without antimatter domains, the presence of distinct domains of matter and antimatter in the Dirac-Milne cosmology provides a natural scenario for the production of D and ${}^3\text{He}$ in a second stage of nucleosynthesis.

4.2. Secondary production of D and ${}^3\text{He}$

Studies of inhomogeneous big-bang nucleosynthesis as well as primordial nucleosynthesis in presence of matter and antimatter domains have been conducted since the late 70's (Combes et al. 1975; Aly 1978a; Witten 1984; Alcock et al. 1987; Applegate et al. 1987; Kurki-Suonio & Sihvola 2000; Rehm & Jedamzik 2001). It has been shown that matter-antimatter annihilations at the frontiers of the domains can lead to the production of D, ${}^3\text{He}$ and T (later decaying in ${}^3\text{He}$) mainly through two channels of production: nucleodisruption ($\bar{p}{}^4\text{He}$ and ${}^4\text{He}\bar{H}$ reactions) and photodisintegration of ${}^4\text{He}$ nuclei. These studies provide us with the necessary material to compute the amount of deuterium produced by these various mechanisms.

Our purpose in what follows is to demonstrate the possibility of deuterium secondary production. We therefore consider that the emulsion has a static behavior, in the sense that its comoving size is assumed to remain constant. More precise studies investigating the dynamical behavior of the emulsion are beyond the scope of this first paper and will be treated in upcoming works.

Annihilations at the frontiers of a domain are driven by the diffusion of nuclei towards the frontiers. Photodisintegration of ${}^4\text{He}$ nuclei by energetic photons resulting from electromagnetic cascades induced by the annihilation photons and nucleodisruption are two possible processes that could produce deuterium.

The main quantity to consider is the diffusion length. It represents the average distance over which a (anti-)nucleus can dif-

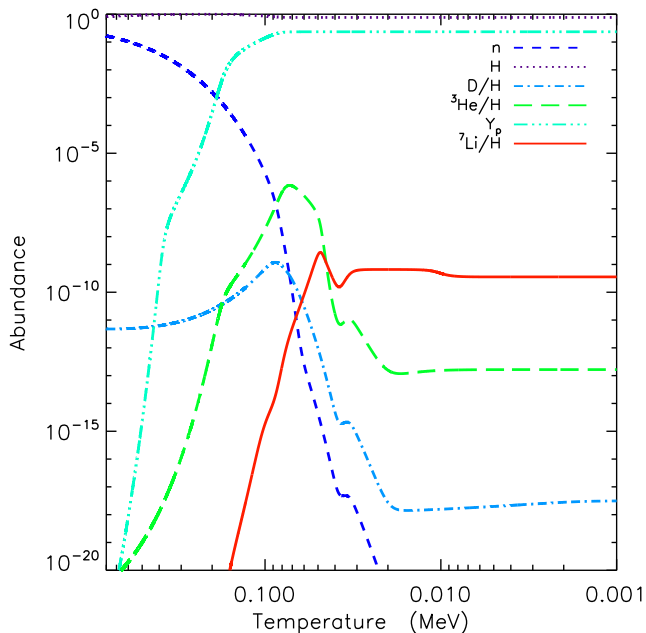


Fig. 5. Abundances of light elements obtained in the Milne Universe with a baryon to photon ratio $\eta = 8.8 \times 10^{-9}$. ${}^4\text{He}$ and ${}^7\text{Li}$ are produced at observationally compatible levels (see Fig. 4), but D and ${}^3\text{He}$ are almost totally destroyed by the very slow thermal nucleosynthesis.

fuse toward the frontier of the domain on a Hubble time. This length gives an absolute lower bound to the size of the domains, as any concentration of (anti)matter smaller than this diffusion length would be annihilated during a Hubble time. The diffusion length reads (Applegate et al. 1987):

$$L_{\text{diff}}(T) = \sqrt{6D(T)t_H(T)}, \quad (13)$$

where D is the diffusion coefficient and $t_H(T)$ is the Hubble time at temperature T . Using the diffusion coefficients given in Jedamzik & Rehm (2001); Sihvola (2001), we computed the comoving diffusion length as represented in Fig. 6.

We can distinguish three regimes of diffusion. The first regime, for $T \geq 1$ MeV is regulated by neutron diffusion. Being neutral particles, their electromagnetic interactions with other charged particles are very weak. As the temperature decreases, neutrons disintegrate and diffusion is then maintained by protons, which being charged present a much lower diffusion coefficient leading to the dip in the diffusion length around 100 keV. As the density decreases because of the expansion, the diffusion length gradually increases until the temperature reaches $T \sim 50$ keV. At that temperature, the density is low enough so that the mean distance between protons is larger than the Debye length of electrons. Protons therefore do not behave as free particles but drag along them electrons, ensuring charge neutrality. These electrons are themselves subject to Thomson drag (Peebles 1993) and thus limit the diffusion of protons (Jedamzik & Rehm 2001). The effective diffusion coefficient of protons is then:

$$D_p^{\text{eff}} = \frac{3T}{2\sigma_T\rho_\gamma}, \quad (14)$$

where σ_T is the Thomson cross-section and ρ_γ , the photon energy density.

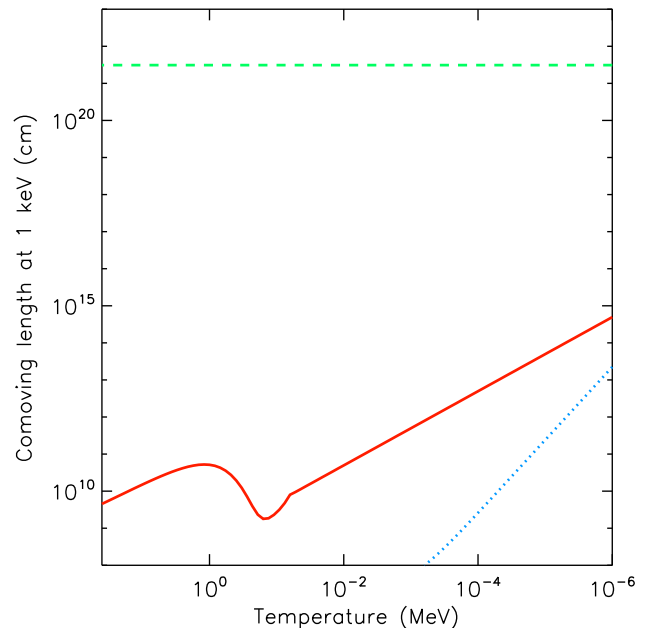


Fig. 6. Comoving diffusion length (solid red line). The blue dashed line is the comoving thermalizing length of deuterium. Comoving Hubble distance is also shown in green.

4.2.1. Annihilation rate

In the most general case, the computation of the annihilation rate is a difficult task (Aly 1978b). However, with our simplified approach based on diffusion, the estimation of the annihilation rate is rather straightforward. The annihilation rate is the number of annihilations per unit of time and surface. The quantity of matter (and of antimatter) annihilated on a Hubble time **per unit of surface** is $n_b L_{\text{diff}}$, so that the annihilation rate is simply this quantity divided by the Hubble time:

$$\Psi = \frac{n_b L_{\text{diff}}}{t_H}. \quad (15)$$

This simple expression is found to be in good agreement with the one derived in Cohen et al. (1998). For simplicity, and following previous studies on antimatter BBN (Kurki-Suonio & Sihvola 2000; Rehm & Jedamzik 2001), we have made the hypothesis that hydrodynamic turbulence, that could be produced by energy release near the domain boundary, can be neglected.

4.2.2. Production by photodisintegration of ${}^4\text{He}$ nuclei

The secondary production of light elements by ${}^4\text{He}$ photodisintegration can occur in many scenarios and has been extensively discussed in the literature. In the framework of standard cosmology, this mechanism is known to produce D and ${}^3\text{He}$ nuclei (Ellis et al. 1992; Protheroe et al. 1995).

Proton-antiproton annihilations result in the production of neutral pions, themselves decaying to high-energy photons. Depending on the temperature of the background and on their energy, these photons can create e^+e^- pairs on CMB-photons. These newly created pairs can also interact with CMB photons and therefore lead to the creation of electromagnetic cascades (Ellis et al. 1992; Protheroe et al. 1995). These cascades stop when the energy of a photon becomes lower than the pair creation threshold $E_{\text{pair}} = m_e^2/E_\gamma$, where E_γ is the energy of a

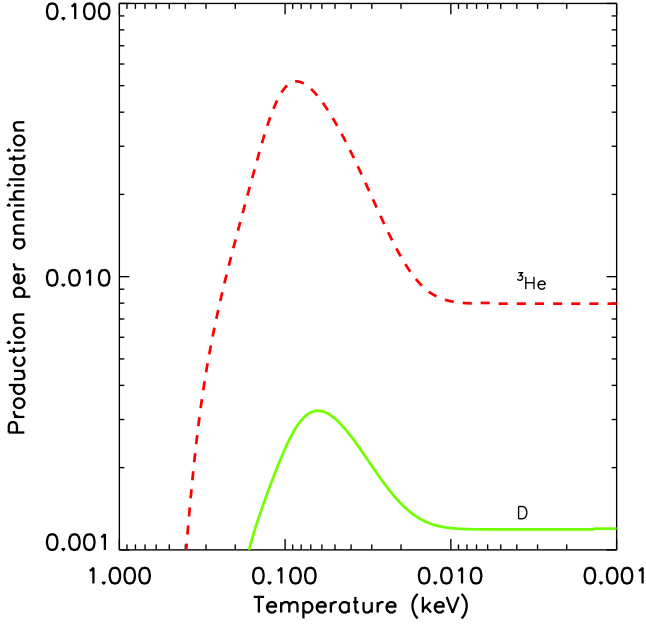


Fig. 7. Quantity of D (solid green) and ${}^3\text{He}$ (dashed red) nuclei produced by ${}^4\text{He}$ nuclei photodisintegration for one $p\bar{p}$ annihilation.

thermal photon. Due the high number of thermal photons, the threshold energy for pair creation is $E_{\text{max}} \sim m_e^2/22T$ (Ellis et al. 1992). Photons with energy lower than E_{max} but higher than $E_c \sim m_e^2/80T$ also undergo elastic scattering on background photons (Svensson & Zdziarski 1990). The resulting spectrum of cascaded photons can be parametrized by (Ellis et al. 1992; Kurki-Suonio & Sihvola 2000):

$$\left. \frac{dn_\gamma}{dE} \right|_{\text{cas}} = \begin{cases} A(E/E_c)^{-1.5}, & E < E_c \\ A(E/E_c)^{-5}, & E_c < E < E_{\text{max}} \\ 0, & E > E_{\text{max}} \end{cases}, \quad (16)$$

where $A = 3E_0E_c^{-2}/[7 - (E_c/E_{\text{max}})^3]$ is a normalization constant, and E_0 is the total energy injected.

Photodisintegration reactions (${}^4\text{He}(\gamma, p){}^3\text{H}$, ${}^4\text{He}(\gamma, n){}^3\text{He}$ and ${}^4\text{He}(\gamma, np)\text{D}$) require photons with energy higher than the respective threshold energies $Q_{{}^4\text{He}(\gamma, np)\text{D}} = 26.07$ MeV, $Q_{{}^4\text{He}(\gamma, p){}^3\text{H}} = 19.81$ MeV and $Q_{{}^4\text{He}(\gamma, n){}^3\text{He}} = 20.58$ MeV (Cyburt et al. 2003). The existence of these threshold energies implies that photodisintegration is a late process, as it becomes efficient only when E_{max} becomes larger than one of the previous threshold values. This happens at a temperature $T_{\text{ph}} \sim 0.5$ keV.

High-energy photons responsible for ${}^4\text{He}$ photodisintegration mainly interact with ambient electrons through Compton scattering or with ambient nuclei through Bethe-Heitler process (Jedamzik 2006). Taking that into account, the number of D nuclei produced per $p\bar{p}$ annihilation reads:

$$N_{\text{D}} = \int_{Q_{\text{D}}}^{E_{\text{max}}} dE_\gamma \frac{n_\alpha \sigma_{{}^4\text{He}(\gamma, np)\text{D}}(E_\gamma)}{f(E_\gamma)} \left. \frac{dn_\gamma}{dE_\gamma} \right|_{\text{tot}}, \quad (17)$$

in which $f(E_\gamma) = n_p \sigma_{\text{BH}}(E_\gamma, 1) + n_\alpha \sigma_{\text{BH}}(E_\gamma, 2) + k(E_\gamma) n_e \sigma_{\text{KN}}(E_\gamma)$, where σ_{BH} is the Bethe-Heitler process cross-section, σ_{KN} the Compton scattering cross-section in the Klein-Nishina regime (Rybicki & Lightman 1979) and $k(E_\gamma) \approx 1 - 4/3[\ln(2E_\gamma/m_e) + 1/2]^{-1}$ is the mean fractional

energy loss by Compton scattering (Protheroe et al. 1995). A similar formula exists for ${}^3\text{He}$. Figure 7 presents the results of this calculation.

When photodisintegration is most effective (around $T \sim 100$ eV), the mean free path of high energy photons relative to these processes is higher than the diffusion length, implying that D and ${}^3\text{He}$ nuclei produced by photodisintegration will be able to survive and will add to the overall light elements production. More precisely, one can estimate the temperature (or equivalently the redshift) from which newly produced nuclei will not be annihilated later on. It is then necessary to assume that there exists a redshift z_{end} where matter and antimatter cease to annihilate. The hypothesis of gravitational repulsion between matter and antimatter leads to this *gravitational decoupling* but the exact mechanism, which would be analogous to the separation of electrons and holes in a gravitational field remains to be demonstrated. We emphasize that this decoupling is a necessary condition for the viability of the Dirac-Milne model. A theoretical determination of z_{end} appears to be possible by analogy with the electron-hole system (Tsidil'kovskii 1975), but we leave it here as a free parameter which will be later constrained by observations. Let us note $L_{\text{diff}}^{z_{\text{end}}}(z)$ the comoving value, calculated at a redshift z , of the diffusion length at redshift z_{end} . We have:

$$L_{\text{diff}}^{z_{\text{end}}}(z) = L_{\text{diff}}(z_{\text{end}}) \left(\frac{1+z}{1+z_{\text{end}}} \right). \quad (18)$$

Any nuclei produced at a distance from the domain boundary smaller than this length will be annihilated by z_{end} , whereas nuclei produced farther will survive once annihilation stops. We can then determine the redshift z_* below which high energy photons mean free path is larger than $L_{\text{diff}}^{z_{\text{end}}}(z_*)$. z_* is then the redshift below which D and ${}^3\text{He}$ nuclei produced by photodisintegration will add up to the final abundances.

Multiplying (17) by the annihilation rate and integrating between the times corresponding to z_* and z_{end} , we get N_{D}^{ph} , the number of D nuclei produced by photodisintegration of ${}^4\text{He}$ nuclei:

$$N_{\text{D}}^{\text{ph}} = \frac{1}{H_0} \int_{z_*}^{z_{\text{end}}} N_{\text{D}}(z) \Psi(z) S(z) \frac{dz}{(1+z)^2}. \quad (19)$$

We can get rid of the surface term $S(z)$ by dividing eq. (19) by the total number of baryons in the volume V , $n_b V$, which yields the final D abundance:

$$\left. \frac{\text{D}}{\text{H}} \right|_{\text{ph}} = \left(\frac{T_0}{1 \text{ keV}} \right) \frac{1}{L_{1\text{keV}}} \int_{z_*}^{z_{\text{end}}} L_{\text{diff}}(z) N_{\text{D}} dz. \quad (20)$$

This expression only depends on two variables, z_{end} , the redshift of gravitational decoupling and $L_{1\text{keV}}$, the comoving emulsion size at 1 keV. The values of the final D and ${}^3\text{He}$ abundances as a function of these two parameters are presented on Fig. 8.

Electromagnetic cascades initiated by annihilation photons cause the injection of non-thermal energy into the background radiation. In the standard cosmology, these energy injections are severely constrained, notably by the FIRAS measurements (Fixsen et al. 1996). However, in the Dirac-Milne universe, due to the slow value of the expansion rate, the radiative processes that can thermalize virtually any energy injection (Danese & de Zotti 1977; Hu & Silk 1993) decouple at a lower redshift than in the standard case. The detailed calculation of the thermalization of CMB distortions will be presented elsewhere, but the exclusion contour in the $(z_{\text{end}} - L_{1\text{keV}})$ plane is shown in Fig. 8.

In order to have a final D abundance in agreement with observations ($\text{D}/\text{H} \sim 3 \times 10^{-5}$, Pettini et al. 2008) and imposing

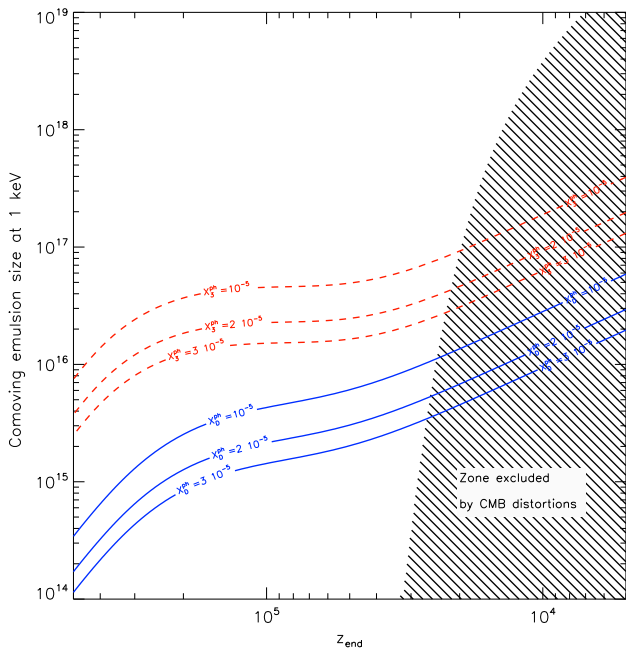


Fig. 8. D and ${}^3\text{He}$ final abundance as a function of the size of the emulsion and the redshift of gravitational decoupling. Hatched region is forbidden because of CMB distortions constraints.

the gravitational decoupling as late as possible, we find that the comoving size of the domains at 1 keV has to be around:

$$L_{1\text{keV}} \sim 10^{15} \text{ cm}, \quad (21)$$

which corresponds to a size of 7 kpc comoving today. This estimate of the size of the emulsion may seem small compared, for instance, to the typical size of a galaxy, implying that there should exist numerous matter and antimatter domains inside a single galaxy. However, it is to be reminded that this size is only constrained when gravitational decoupling occurs and that domains, which are in a non linear mode of evolution immediately after photon matter-radiation decoupling, will have a dynamical behavior after recombination that leads to an effective increase of that size (Dubinski et al. 1993; Piran 1997).

As suggested by Fig. 7, secondary production of light elements by photodisintegration of ${}^4\text{He}$ leads to an overproduction of ${}^3\text{He}$ compared to D. Indeed, it is usually considered that D can only be destroyed by stellar processes. On the other hand, ${}^3\text{He}$ can be produced or destroyed, but the ratio D/ ${}^3\text{He}$ can only decrease (Sigl et al. 1995). As this ratio is observed in our Galaxy to be D/ ${}^3\text{He} \sim 1$ and since this ratio is predicted to be D/ ${}^3\text{He} \sim 0.1$ in the Dirac-Milne universe, the overproduction of ${}^3\text{He}$ is a priori a serious constraint on the Dirac-Milne model. However, it has been noted (see Jedamzik (2002) for a review) that D enhancement could happen at high redshift and could therefore alleviate the ${}^3\text{He}$ constraint.

4.2.3. Production by nucleodisruption

Nucleodisruption has been found to be an important source of D and ${}^3\text{He}$ nuclei (Sihvola 2001) within the standard evolution of the scale factor. However, with the slow evolution of the expansion rate in the Dirac-Milne universe and with the hypothesis we made on the spatial repartition of matter and antimatter domains, this situation changes.

Nuclei produced by nucleodisruption possess a kinetic energy ranging from a few MeV for nuclei to a few dozens of MeV for nucleons (Balestra et al. 1988). These newly produced nuclei thermalize by Coulomb scattering on ambient protons and electrons. The thermalization length for D nuclei produced with an energy $E_0 = 10$ MeV is presented in Fig. 6 (blue dotted line). This distance is always much smaller than the diffusion length, implying that any D nucleus produced by nucleodisruption will finally return towards the annihilation zone and be destroyed there. A possible way to produce a higher fraction of deuterium by nucleodisruption would be to consider small domains of (anti)matter inside a bigger domain of antimatter (matter). This situation occurs continually in an emulsion, which suffers a redistribution of “domains” when bridges in the emulsion disappear by annihilation. If the dimension of the larger domain is larger than the diffusion length, then an important fraction of the D and ${}^3\text{He}$ produced by nucleodisruption could survive. However, precise calculations of this production requires the knowledge of the statistical properties of the spatial distribution of domains, which strongly depends of the separation mechanism. This point should be investigated in future studies of nucleosynthesis in the Dirac-Milne universe.

5. Type Ia supernovæ

In 1998 (Riess et al. 1998; Perlmutter et al. 1999), distance measurements on Type Ia Supernovæ (SNe Ia) have revealed that these objects are dimmer than expected if our Universe was correctly described by a decelerating Einstein-de Sitter model. The introduction of a cosmological constant Λ in the field equations of General Relativity, apt to produce an accelerating expansion, proved to give an impressive fit to the observational data. Today, SNe Ia are one of the most important cosmological tests and are considered as the prime evidence for an acceleration of the expansion. It should be reminded however that the strong evidence for a recent transition between a decelerating phase and an accelerating phase of expansion heavily relies on the prior hypothesis of spatial flatness. Without this hypothesis, the evidence is less clear (Seikel & Schwarz 2008).

The Dirac-Milne universe does not present any acceleration nor deceleration and is therefore equivalent to an open empty universe. In terms of usual cosmological parameters, this universe corresponds to the following combination:

$$(\Omega_M = 0, \Omega_\Lambda = 0). \quad (22)$$

In this context, luminosity distance in the Dirac-Milne universe take the following simple expression :

$$d_L(z) = \frac{c}{H_0} (1+z) \sinh[\ln(1+z)]. \quad (23)$$

It is usually claimed that the empty universe, hence the Dirac-Milne universe is strongly rejected by the SNe Ia observations. We wish here to precise this statement using the data of the first release of the SNLS collaboration (Astier et al. 2006). The SNLS data consists of two distinct datasets. The high-redshift sample comes from the SNLS. It comprises 71 SNe Ia with redshift between $0.2 \leq z \leq 1.01$. The second sample is the low-redshift set, 44 SNe Ia taken from the literature with redshift $z \leq 0.15$. These data come from different experiments and are therefore possibly subject to different sources of systematic errors.

Following the definition given in Astier et al. (2006), the distance modulus is:

$$\mu_B = m_B^* - M + \alpha(s-1) - \beta c, \quad (24)$$

where M is the absolute magnitude of SNe Ia, α and β are global parameters that link the stretch s and the color c to the distance modulus, and m_B^* , the apparent magnitude of the supernova. It should be emphasized that, contrary to the Λ CDM cosmology, there is no cosmological parameter dependence in the Dirac-Milne luminosity distance. The only degrees of freedom come from the nuisance parameters, M , α and β . Following the procedure described in Astier et al. (2006), we minimize the following expression:

$$\chi^2 = \sum \frac{(\mu_B - 5 \log_{10}(d_L/10 \text{ pc}))^2}{\sigma^2(\mu_B) + \sigma_{\text{int}}^2}. \quad (25)$$

Here, $\sigma(\mu_B)$ takes into account measurement errors on the apparent magnitude m_B^* , stretch and color parameters derived by the analysis of light-curves (Guy et al. 2005). σ_{int} is the so called "intrinsic" dispersion, which is a parameter introduced to account for the fact that SNe Ia are astrophysical objects and naturally present some dispersion in their absolute magnitude. However, the value of this parameter is unknown and in the fitting procedure, σ_{int} is adjusted so that the reduced chi-squared is unity.

5.1. Analysis with only the high- z sample

First, we performed our analysis on the high- z sample without including any low- z SN Ia. Without this low- z anchoring, the analysis does not permit to discriminate between the Λ CDM and the Dirac-Milne universes. In this respect, it is important to note that the recent 3-year analysis of SNLS using their data alone (Guy et al. 2010) is consistent at a better than 68% CL with the Dirac-Milne universe, while the Einstein-de Sitter (EdS) model is clearly excluded. The evidence for expansion acceleration therefore relies on a comparison between low- z and high- z SNe Ia. We also present the results for the EdS model.

Table 1. Values of the different parameters for the fit using only the 71 high- z SNe Ia of the SNLS. Here, σ_{int} has been fixed to $\sigma_{\text{int}} = 0$. The number in parenthesis indicates the number of degrees of freedom.

Parameter	Dirac-Milne	Λ CDM	EdS
Ω_M	...	0.289 ± 0.033	1
M	-19.24	-19.36	-19.04
σ_{int}	0	0	0
χ^2 total	553.64	558.6	724.38
χ^2/dof	8.14(68)	8.33 (67)	10.65(68)

Table 2. Values of the different parameters for the fit using only the 71 high- z SNe Ia of the SNLS. Here σ_{int} has been adjusted so that $\chi^2/\text{d.o.f.} = 1$. The number in parenthesis indicates the number of degrees of freedom.

Parameter	Dirac-Milne	Λ CDM	EdS
Ω_M	...	0.25 ± 0.08	1
M	-19.18	-19.33	-18.87
σ_{int}	0.1172	0.1173	0.155
total χ^2	68.01	67.01	67.97
χ^2/dof	1.00 (68)	1.00 (67)	1.0 (68)

Results of the analysis of the 71 SNe Ia are presented in Tables 1 and 2. In Table 1, the intrinsic dispersion is fixed at a null value. The analysis is therefore done with the sole measurements errors, thereby giving a stronger weight to SNe Ia with redshift $0.2 \leq z \leq 0.4$ which present smaller errors. The total and reduced χ^2 of the EdS model are much larger than those of the Λ CDM and Dirac-Milne models, which are in turn similar. In Table 2, the intrinsic dispersion is determined by requiring the condition that the reduced chi-squared is unity. The value of the intrinsic dispersion required to renormalize the reduced χ^2 of the EdS model to unity is here again much larger than those required for the other two models. The conclusion of this first analysis is twofold. First, we confirm that the decelerating Einstein-de Sitter model is disfavoured, which should come as no surprise. Second, the Dirac-Milne and the flat Λ CDM are very close, Dirac-Milne being even slightly better than the flat Λ CDM model. Our analysis stresses the fact that SNe Ia analysis heavily relies on the use of low- z data to anchor the Hubble diagram.

5.2. Analysis on the full data set

Similarly, we proceeded our analysis on the full data sample used by SNLS in its one-year analysis, i.e. using an heterogeneous sample of low- z SNe Ia. Results are given in Tables 3 and 4. In this case, as expected, the flat Λ CDM proves a better fit to the data than the Dirac-Milne universe.

Table 3. Values of the different parameters for the fit using the complete data set of 115 SNe Ia. Here, σ_{int} has been fixed to $\sigma_{\text{int}} = 0$. The number in parenthesis indicates the number of degrees of freedom.

Parameter	Dirac-Milne	Λ CDM	EdS
Ω_M	...	0.258 ± 0.019	1
M	-19.258	-19.38	-19.01
σ_{int}	0	0	0
χ^2 total	877.93	809.75	1507.83
χ^2/dof	7.83 (112)	7.295 (111)	13.46 (112)

Table 4. Values of the different parameters for the fit using the complete data set of 115 SNe Ia. Here σ_{int} has been adjusted so that $\chi^2/\text{d.o.f.} = 1$. The number in parenthesis indicates the number of degrees of freedom.

Parameter	Dirac-Milne	Λ CDM	EdS
Ω_M	...	0.250 ± 0.036	1
M	-19.217	-19.331	-18.98
σ_{int}	0.1432	0.1289	0.258
χ^2 total	112.05	110.96	111.95
χ^2/dof	1.00 (112)	0.99(111)	0.99 (112)

In Fig. 9, we present the residuals of the Hubble diagram for the Dirac-Milne, the flat Λ CDM and Einstein-de Sitter models. The left column represents the residuals when the value of the intrinsic dispersion is adjusted to normalize the χ^2 to 1 per degree of freedom. In the right column, are presented the residuals obtained when the intrinsic dispersion parameter is fixed to the value $\sigma_{\text{int}} = 0$. Setting σ_{int} to 0 enables one to consider the "real" measurement errors. It appears that for the SNe in the

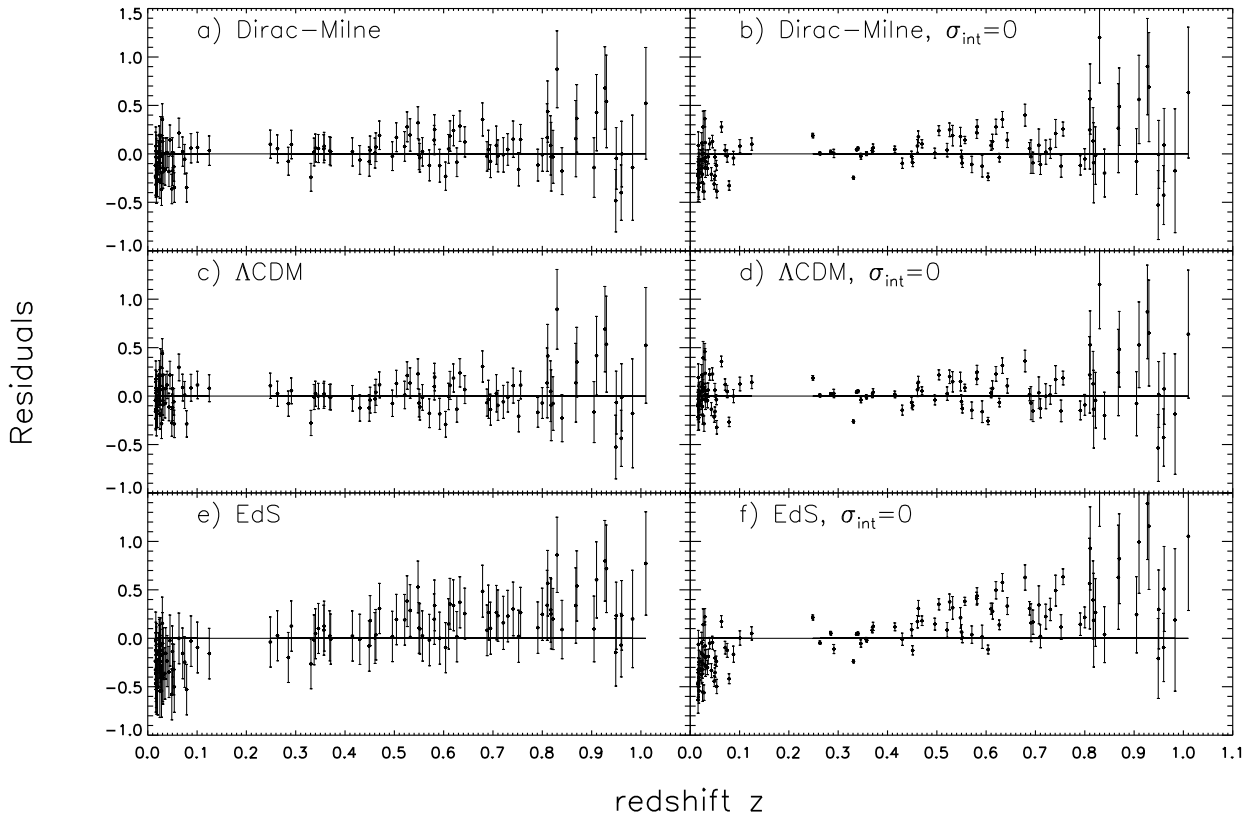


Fig. 9. Residuals of the Hubble diagram for the Dirac-Milne ((a) and (b)), flat Λ CDM ((c) and (d)) and Einstein de-Sitter ((e) and (f)) models. The left column represents the residuals obtained by the minimization of the χ^2 defined by eq. (25), in which the values of the intrinsic dispersion is adjusted so that $\chi^2/\text{d.o.f.} = 1$. In the right column, this intrinsic dispersion is fixed to 0.

range $0.2 \leq z \leq 0.8$ these errors are lower than the intrinsic dispersion. The use of such an ad-hoc parameter in the analysis has for consequence that it possibly degrades the quality of the data in the 0.2-0.4 z interval, where the quality of the observations is highest. Note that such analysis with statistical errors only has been realized in the recent SNLS 3-year analysis (Guy et al. 2010).

Panels e) and f) present the residuals for the Einstein-de Sitter model. Even though the reduced χ^2 has been constrained to unity in panel e), the presence of a characteristic slope in the residuals indicates the non-conformity of the Einstein-de Sitter model to the data. The difference between the Dirac-Milne and the Λ CDM models is however very subtle, and can hardly be seen by simply looking at the residuals.

It should be noted that it is only the use of nearby SNe Ia that enables to distinguish between the Dirac-Milne and the Λ CDM models, which is then favored at more than 3σ as previously announced (Astier et al. 2006; Kowalski et al. 2008).

It is now acquired that sources of previously unaccounted for systematic errors (Kelly et al. 2010) are present in the nearby sample. Within this perspective, we determined the constant offset on the apparent magnitude of nearby SNe Ia required for the chi-squared for the Dirac-Milne and the flat Λ CDM to become equal. We found that an offset of $\delta m_B^* = 0.06$ mag is sufficient to have the two models equally probable. This value should be compared to the budget of systematics errors estimated in recent studies: $\Delta M = 0.04$ mag (Kowalski et al. 2008). Therefore, a relatively mild systematic error of 1.5σ on nearby SNe Ia would

result in favouring the Dirac-Milne universe over the conventional Λ -CDM cosmology in the SNe Ia analysis.

6. Other tests

A major result of CMB experiments was to measure precisely the position of the first acoustic peak at the degree scale, which seems to imply that the spatial curvature is nearly zero (Komatsu et al. 2010). In the open spatial geometry of the Dirac-Milne universe, this position would naively be expected at a much smaller angle. Indeed, the ratio of the angular distances in the two models taken at redshift $z \sim 1100$, which corresponds to the surface of last scattering surface, is:

$$\frac{d_A^{\text{Milne}}(z) \Big|_{z=1100}}{d_A^{\Lambda\text{CDM}}(z)} \stackrel{\#}{=} 169. \quad (26)$$

The value of this ratio implies that an astrophysical object at redshift $z = 1100$ is seen under an angle 169 times smaller in the Dirac-Milne universe than in the Λ CDM cosmology.

The angular position of the first peak is defined by the angle under which the sound horizon is seen at recombination:

$$\theta = \frac{\chi_s(z_*)}{d_A(z_*)}, \quad (27)$$

where $\chi_s(z_*)$ is the sound horizon, $d_A(z_*)$ the angular distance and z_* the redshift of the last scattering surface. It is of interest to consider the equivalent multipole $\ell_a \sim \pi/\theta$. The sound horizon is defined as the distance that acoustic waves can travel in the

primordial plasma. Taking into account the universe expansion, this distance reads:

$$\chi_s = \int_0^t c_s \frac{dt'}{a(t')}, \quad (28)$$

where the speed of sound $c_s = c/\sqrt{3(1+R)}$, R being a corrective factor due to the presence of baryons (Hu & Sugiyama 1995). Its value can be related to the baryon to photon ratio η by $R \approx 1.1 \times 10^{12} \eta / (1+z)$.

The definition of the lower bounds of the integral requires some care as we have shown previously that this integral diverges near the initial singularity. However, the mechanisms of sound generation in the Dirac-Milne and Λ CDM universes differ radically. Contrasting with the generation of sound waves in the Standard Model where inhomogeneities are produced at the epoch of inflation, it seems reasonable to consider that sound waves in the Dirac-Milne universe are probably produced by annihilation at the matter-antimatter frontiers. It is therefore natural to consider for this value the epoch of QGP transition around $T \sim 170$ MeV. Indeed, in the absence of inflation, the universe is very homogeneous before this event, and QGP transition seems naturally to be the scale of interest in the Dirac-Milne cosmology. There exists at present a rather general consensus that the QCD transition is not first or second order at zero chemical potential, but is probably an analytic crossover (see e.g. Aoki et al. (2006); Bazavov et al. (2009); Endrődi et al. (2011) and references therein). Under this hypothesis, it would be extremely difficult, if not impossible, to understand how significant amounts of matter and antimatter could have survived annihilation in the very slow evolution of the Dirac-Milne universe. On the other hand, the present belief is based on a QCD calculation, whereas the situation of the primordial universe is more complicated, including additional light leptons (electrons, positrons, neutrinos and antineutrinos). Also, present calculations use light quark mass for the u and d quarks that are significantly higher than the actual masses of these quarks. Therefore, the observation of large matter-antimatter domains would be an extremely useful indication that, contrary to present expectations, there is a sharp transition allowing the survival of significant regions of antimatter at the QCD transition. It should also be noted that some authors are clearly considering the possibility that baryogenesis occurs at the QCD transition or at a $O(100)$ MeV temperature (see for example Dolgov (1992) for a review).

Acoustic waves then propagate in the plasma as long as matter and antimatter are in contact, *i.e.* until the gravitational decoupling, estimated in the previous section at $z_{end} \approx 3 \times 10^4$. With these values, the comoving sound horizon is found:

$$\chi_s \sim 42 \text{ Gpc}. \quad (29)$$

The expression of the angular position of the first acoustic peak then follows:

$$\ell_a \sim \pi \frac{d_A}{\chi_s(z_*)}, \quad (30)$$

It can be shown that the redshift of last scattering surface in the Dirac-Milne universe is a few percent lower than in the standard cosmology, here again due to the late decoupling of the radiative processes leading to recombination. We found $z_* \sim 1040$.

Calculating the multipole of the acoustic scale using expression (30), we obtain $\ell_a \sim 160$. The standard value of this quantity is $\ell_a \sim 300$ (Spergel et al. 2003). Instead of a discrepancy by a

factor ≈ 169 , there is an almost exact compensation between the larger geometrical term, induced by the open geometry of the Dirac-Milne universe, and the larger sound horizon, caused by the slow evolution of the expansion rate before recombination. Taking into account the numerous approximations in the model, this remarkable coincidence is quite unexpected and represents a fascinating motivation to study in more detail the Dirac-Milne universe.

However the sound horizon scale is also imprinted in the large-scale structure power spectrum under the form of small oscillations (Eisenstein & Hu 1998) called Baryonic Acoustic Oscillations (BAO). These oscillations are expected, at least in first approximation, at the same scale as the sound horizon. As discussed above, the sound horizon is much larger in the Dirac-Milne universe than in the Standard Cosmology. Admitting that there are BAOs in the Dirac-Milne universe, they should be expected at a scale much larger than that of the standard Cosmology. The claimed detection of these BAOs at the expected scale (within the standard cosmology) of ~ 150 Mpc (Eisenstein et al. 2005), presently detected at the $\sim 3\sigma$ level, if confirmed by ongoing experiments, would therefore pose a severe constraint on the Dirac-Milne universe.

7. Conclusion

Motivated by the puzzling situation in cosmology, where the standard Λ CDM model is in good agreement with observations but rather poorly theoretically motivated, we have studied an alternative cosmological model, the Dirac-Milne universe. Inspired by the work of Dirac, Kerr and Carter, this model restores the symmetry between matter and antimatter. Relying on the symmetries of the Kerr-Newman solutions in General Relativity, it makes the hypothesis that particles and antiparticles behave similarly to quasiparticles such as electrons and holes in a semiconductor, and that antimatter has a negative active gravitational mass. A fundamental characteristic of this Universe is the linear evolution of its scale factor that solves in an elegant way both the horizon and the age of the universe problems.

Concerning primordial nucleosynthesis, we have found that the Dirac-Milne universe is able to produce ${}^4\text{He}$ at an adequate level, while producing ${}^7\text{Li}$ nuclei in proportions admittedly a factor 3 higher than the observed values but with a lower tension between observations and predictions compared to the standard cosmology. We have also shown that surface annihilations at the frontiers of matter and antimatter naturally lead to the production of D nuclei, in a quantity which is proportional to the inverse of the characteristic size of the emulsion. Our main concern in this work was the production of D, and for that purpose the assumption of a fixed characteristic size of the emulsion is clearly an approximation. Relaxing this assumption will allow the possibility of the total annihilation of small patches of antimatter inside larger regions of matter. This might lead to a net production of D by nucleodisruption, which has a higher D/ ${}^3\text{He}$ production ratio (Balestra et al. 1988), therefore alleviating the constraints posed by overproduction of ${}^3\text{He}$ nuclei.

The Dirac-Milne universe does not present an accelerated expansion and seems therefore in opposition with the usual interpretation of Type Ia distance measurements. We have shown that the Dirac-Milne universe can nevertheless be reconciled with Type Ia supernovae observations if we take into account a reasonable amount of systematic errors on the low- z supernovae subset. Finally, and perhaps the most surprising result about this unusual cosmology is that the acoustic scale naturally emerges at the degree scale, despite an open geometry.

These first results are encouraging but some possible tension points have not been covered by this study. Amongst these, structure formation in presence of separate domains of positive and negative mass is a crucial question. Use of numerical simulations will most probably be a necessity as the usual linear approximation does not hold. Indeed, immediately after matter-radiation decoupling, density contrast is of order unity for any distribution of matter with positive mass and antimatter with negative mass.

Acknowledgments

It is a pleasure to acknowledge fruitful discussions with J. Andrea, E. Armengaud, B. Carter, N. Fourmanoit, J. Fric, K. Jedamzik, T. Jolicœur, E. Keihänen, R. Pain, J. Rich and the members of the SNLS collaboration. Special thanks to A. Coc for allowing us to adapt his nucleosynthesis code. Needless to say, these people are not responsible for the errors present in this, admittedly provoking but hopefully interesting, paper.

References

- Alcock, C., Fuller, G. M., & Mathews, G. J. 1987, *Astrophys. J.*, 320, 439
- Aly, J. J. 1974, *Astron. & Astrophys.*, 35, 311
- Aly, J. J. 1978a, *Astron. & Astrophys.*, 64, 273
- Aly, J. J. 1978b, *Astron. & Astrophys.*, 67, 199
- Angulo, C., Arnould, M., Rayet, M., et al. 1999, *Nuclear Physics A*, 656, 3
- Aoki, Y., Endrődi, G., Fodor, Z., Katz, S. D., & Szabó, K. K. 2006, *Nature*, 443, 675
- Applegate, J. H., Hogan, C. J., & Scherrer, R. J. 1987, *Phys. Rev. D*, 35, 1151
- Arcos, H. I. & Pereira, J. G. 2004, *General Relativity and Gravitation*, 36, 2441
- Astier, P., Guy, J., Regnault, N., et al. 2006, *Astron. & Astrophys.*, 447, 31
- Balestra, F., Bossolasco, S., Bussa, M. P., et al. 1988, *Nuovo Cimento A Serie*, 100, 323
- Bazavov, A., Bhattacharya, T., Cheng, M., et al. 2009, *Phys. Rev. D*, 80, 014504
- Bregman, J. N. 2007, *Ann. Rev. Astron. Astrophys.*, 45, 221
- Burinskii, A. 2008, *Gravitation and Cosmology*, 14, 109
- Carter, B. 1968, *Physical Review*, 174, 1559
- Caughlan, G. R. & Fowler, W. A. 1988, *Atomic Data and Nuclear Data Tables*, 40, 283
- Chaboyer, B., Demarque, P., Kernan, P. J., & Krauss, L. M. 1998, *Astrophys. J.*, 494, 96
- Chardin, G. 1997, *Hyperfine Interactions*, 109, 83
- Chardin, G. & Rax, J.-M. 1992, *Physics Letters B*, 282, 256
- Chen, J.-W. & Savage, M. J. 1999, *Phys. Rev. C*, 60, 065205
- Coc, A., Hernanz, M., José, J., & Thibaud, J.-P. 2000, *Astron. & Astrophys.*, 357, 561
- Cohen, A. G., de Rujula, A., & Glashow, S. L. 1998, *Astrophys. J.*, 495, 539
- Combes, F., Fassi-Fehri, O., & Leroy, B. 1975, *Astrop. & Sp. Sci.*, 37, 151
- Cybur, R. H., Ellis, J., Fields, B. D., & Olive, K. A. 2003, *Phys. Rev. D*, 67, 103521
- Cybur, R. H., Fields, B. D., & Olive, K. A. 2008, *Journal of Cosmology and Astro-Particle Physics*, 11, 12
- Danese, L. & de Zotti, G. 1977, *Nuovo Cimento Rivista Serie*, 7, 277
- Descouvemont, P., Adahchour, A., Angulo, C., Coc, A., & Vangioni-Flam, E. 2004, *Atomic Data and Nuclear Data Tables*, 88, 203
- Dicus, D. A., Kolb, E. W., Gleeson, A. M., et al. 1982, *Phys. Rev. D*, 26, 2694
- Dolgov, A. D. 1992, *Physics Reports*, 222, 309
- Drobychev, G. Y., Ndlec, P., Sillou, D., et al. 2007, Proposal for the AEGIS experiment at the CERN antiproton decelerator (Antimatter Experiment: Gravity, Interferometry, Spectroscopy), Tech. Rep. SPSC-P-334. CERN-SPSC-2007-017, CERN, Geneva
- Dubinski, J., da Costa, L. N., Goldwirth, D. S., Lecar, M., & Piran, T. 1993, *ApJ*, 410, 458
- Eisenstein, D. J. & Hu, W. 1998, *Astrophys. J.*, 496, 605
- Eisenstein, D. J., Zehavi, I., Hogg, D. W., et al. 2005, *Astrophys. J.*, 633, 560
- Ellis, J., Gelmini, G. B., Lopez, J. L., Nanopoulos, D. V., & Sarkar, S. 1992, *Nuclear Physics B*, 373, 399
- Endrődi, G., Fodor, Z., Katz, S. D., Szabó, & K. K. 2011, *Journal of High Energy Physics*, 4, 1
- Fixsen, D. J., Cheng, E. S., Gales, J. M., et al. 1996, *Astrophys. J.*, 473, 576
- Fixsen, D. J. & Mather, J. C. 2002, *Astrophys. J.*, 581, 817
- Fukugita, M. 2004, in *IAU Symposium*, Vol. 220, *Dark Matter in Galaxies*, ed. S. Ryder, D. Pisano, M. Walker, & K. Freeman, 227–+
- Fukugita, M. & Kajino, T. 1990, *Phys. Rev. D*, 42, 4251
- Guy, J., Astier, P., Nobili, S., Regnault, N., & Pain, R. 2005, *Astron. & Astrophys.*, 443, 781
- Guy, J., Sullivan, M., Conley, A., et al. 2010, *ArXiv e-prints*
- Hawking, S. W. 1965, *Royal Society of London Proceedings Series A*, 286, 313
- Hoyle, F. & Narlikar, J. V. 1964, *Royal Society of London Proceedings Series A*, 282, 191
- Hu, W. & Silk, J. 1993, *Phys. Rev. D*, 48, 485
- Hu, W. & Sugiyama, N. 1995, *Astrophys. J.*, 444, 489
- Jedamzik, K. 2002, *Planet. Space Sci.*, 50, 1239
- Jedamzik, K. 2006, *Phys. Rev. D*, 74, 103509
- Jedamzik, K. & Rehm, J. B. 2001, *Phys. Rev. D*, 64, 023510
- Kaplinghat, M., Steigman, G., Tkachev, I., & Walker, T. P. 1999, *Phys. Rev. D*, 59
- Kaplinghat, M., Steigman, G., & Walker, T. P. 2000, *Phys. Rev. D*, 61, 103507
- Kelly, P. L., Hicken, M., Burke, D. L., Mandel, K. S., & Kirshner, R. P. 2010, *Astrophys. J.*, 715, 743
- Komatsu, E., Smith, K. M., Dunkley, J., et al. 2010, *ArXiv e-prints*
- Kowalski, M., Rubin, D., Aldering, G., et al. 2008, *Astrophys. J.*, 686, 749
- Kurki-Suonio, H. & Sihvola, E. 2000, *Phys. Rev. D*, 62, 103508
- Lohiya, D., Batra, A., Mahajan, S., & Mukherjee, A. 1998, *ArXiv General Relativity and Quantum Cosmology e-prints*
- Milne, E. A. 1933, *Zeitschrift für Astrophysik*, 6, 1
- Olive, K. A. & Skillman, E. D. 2004, *Astrophys. J.*, 617, 29
- Omnès, R. 1972, *Phys. Rep.*, 3, 1
- Peebles, P. J. E. 1993, *Principles of physical cosmology (Princeton Series in Physics, Princeton, NJ: Princeton University Press, —c1993)*
- Pérez, P., Liszkay, L., Barthe, M. F., et al. 2008, in *American Institute of Physics Conference Series*, Vol. 1037, *American Institute of Physics Conference Series*, ed. Y. Kanai & Y. Yamazaki, 35–42
- Perlmutter, S., Aldering, G., Goldhaber, G., et al. 1999, *Astrophys. J.*, 517, 565
- Pettini, M., Zych, B. J., Murphy, M. T., Lewis, A., & Steidel, C. C. 2008, *MNRAS*, 391, 1499
- Pfenniger, D., Combes, F., & Martinet, L. 1994, *Astron. & Astrophys.*, 285, 79
- Piran, T. 1997, *General Relativity and Gravitation*, 29, 1363
- Protheroe, R. J., Stanev, T., & Berezhinsky, V. S. 1995, *Phys. Rev. D*, 51, 4134
- Ramani, A. & Puget, J. L. 1976, *Astron. & Astrophys.*, 51, 411
- Rauscher, T., Applegate, J. H., Cowan, J. J., Thielemann, F.-K., & Wiescher, M. 1994, *Astrophys. J.*, 429, 499
- Rehm, J. B. & Jedamzik, K. 2001, *Phys. Rev. D*, 63, 043509
- Riess, A. G., Filippenko, A. V., Challis, P., et al. 1998, *Astron. J.*, 116, 1009
- Ryan, S. G., Beers, T. C., Olive, K. A., Fields, B. D., & Norris, J. E. 2000, *Astrophys. J. Lett.*, 530, L57
- Rybicki, G. B. & Lightman, A. P. 1979, *Radiative processes in astrophysics (New York, Wiley-Interscience, 1979. 393 p.)*
- Schwarz, D. J. 2003, *Annalen der Physik*, 515, 220
- Seikel, M. & Schwarz, D. J. 2008, *Journal of Cosmology and Astro-Particle Physics*, 2, 7
- Sethi, G., Dev, A., & Jain, D. 2005, *Physics Letters B*, 624, 135
- Sigl, G., Jedamzik, K., Schramm, D. N., & Berezhinsky, V. S. 1995, *Phys. Rev. D*, 52, 6682
- Sihvola, E. 2001, *Phys. Rev. D*, 63, 103001
- Spergel, D. N., Verde, L., Peiris, H. V., et al. 2003, *Astrophys. J. Suppl. Ser.*, 148, 175
- Steigman, G. 2007, *Annual Review of Nuclear and Particle Science*, 57, 463
- Svensson, R. & Zdziarski, A. 1990, *Astrophys. J.*, 349, 415
- Tang, X., Azhari, A., Gagliardi, C. A., et al. 2003, *Phys. Rev. C*, 67, 015804
- Tsidil'kovskii, I. M. 1975, *Soviet Physics Uspekhi*, 18, 161
- Wagoner, R. V. 1969, *Astrophys. J. Suppl. Ser.*, 18, 247
- Witten, E. 1984, *Phys. Rev. D*, 30, 272